JACS
JOURNAL OF THE AMERICAN CHEMICAL SOCIETY

ARTICLE

pubs.acs.org/JACS

Structure−Mechanochemical Activity Relationships for Cyclobutane Mechanophores

Matthew J. Kryger, Alexander M. Munaretto, and Jeffrey S. Moore*

Department of Chemistry and the Beckman Institute of Advanced Science and Technology, University of Illinois at Urbana−Champaign, Urbana, Illinios 61801, United States

Supporting Information

ABSTRACT: Ultrasound activation of mechanophores embedded in polymer backbones has been extensively studied of late as a method for realizing chemical reactions using force. To date, however, there have been few attempts at systematically investigating the effects of mechanophore structure upon rates of activation by an acoustic field. Herein, we develop a method for comparing the relative reactivities of various cyclobutane mechanophores. Through the synthesis and ultrasonic irradiation of a molecular weight series of poly(methyl acrylate) polymers in which each macromolecule has a single chain-centered mechanophore, we find measurable and statistically significant shifts in molecular weight thresholds for mechanochemical activation that depend on the structure of the mechanophore. We also show that calculations based on the constrained geometries simulate external force method reliably predict the trends in mechanophore reactivity. These straightforward calculations and the experimental methods described herein may be useful in guiding the design and the development of new mechanophores for targeted applications.

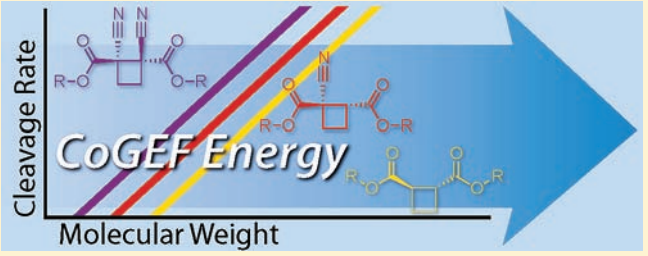

INTRODUCTION

Developing pharmaceutically active molecules is a lengthy and difficult process with the average time from conception to FDA approval being upward of 12 years.[1] One method utilized in the pharmaceutical world to reduce this time and aid in the targeted development of biologically active molecules is the study of structure−activity relationships (SARs).[2] SARs are commonly used to correlate the three-dimensional chemical structure of a molecule and its particular biological function. Utilizing both computational modeling and biological assays, SARs are pharmacophore models for the design of more active and specific biological molecules. However, a method comparable to SAR has never, to our knowledge, been utilized in the growing field of mechanochemistry. Therefore, we considered the possibility of applying a similar approach, structure−mechanochemical activity relationships (SMARs), to probe the importance of chemical structure on mechanophore reactivity and streamline the development of force-sensitive target mechanophores. Lessons learned from the systematic study of a series of properly chosen molecular structures will further increase our understanding of force-activated reactions and improve predictive capabilities for mechanophore design.

While there has been a long-standing interest in mechanically induced reactions in polymers,[3−15] the past five years has seen an increased focus on the development of novel mechanophores with a variety of functional targets including, but not limited to, damage detection through color change,[16−20] self-healing applications,[21,22] and novel reactivity[23−26] as well as mechanically induced polymerizations and catalysis,[27,28] among others.[29−31] While computational modeling has made an impact on our understanding of mechanical activation,[8,19,26,32−39] predicting the ability of mechanophores to undergo mechanically induced reactions, in addition to predicting relative chemical reactivities, has been limited. Here we aim to experimentally validate a simple computational technique, constrained geometries simulate external force (CoGEF),[38] for predicting mechanophore reactivity trends. Experimental validation involved the synthesis and sonication of a molecular weight series of mechanophore-linked polymers to compare their relative rates of reactivity. This paper thus illustrates an example of SMARs and suggests its potential as a useful technique for the rational development of mechanophores with a range of applications and uses.

RESULTS AND DISCUSSION

In order to probe the effects of molecular structure on the fragmentation rates of different mechanophores, six cyclobutanes of varying stereochemistry, electronic environment, and levels of substitution were targeted. It has previously been shown with a small number of examples that substituted cyclobutanes can be sonochemically or mechanically cleaved in a manner consistent with a formal retro [2 + 2] reaction to yield reactive alkenes.[21,40,41] Building on this knowledge, we focused our attention on the cis and trans (with respect to the pendant ester groups) stereoisomers

Received: September 14, 2011
Published: October 27, 2011

dx.doi.org/10.1021/ja2086728 | J. Am. Chem. Soc. 2011, 133, 18992–18998

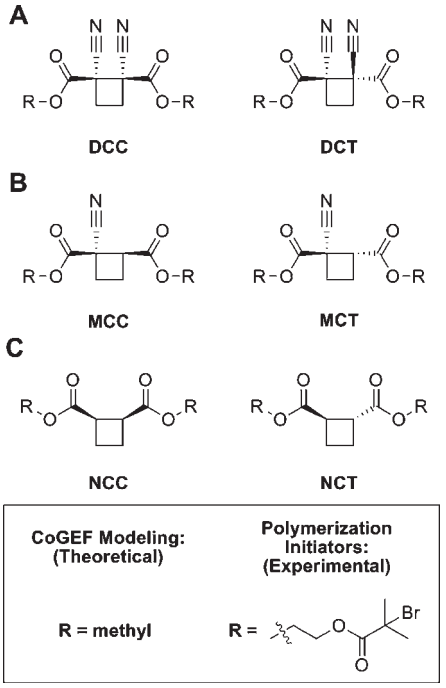

Figure 1. Structures of (A) cis and trans dicyano-substituted cyclobutanes (DCC and DCT), (B) cis and trans monocyano-substituted cyclobutanes (MCC and MCT), and (C) cis and trans cyclobutanes having no cyano substituents (NCC and NCT).

of 1,2-dicyano-substituted cyclobutane (DCC and DCT, respectively, Figure 1A) and the cis and trans stereoisomers of monocyano-substituted cyclobutane (MCC and MCT, Figure 1B) as well as the cis and trans stereoisomers of cyclobutane having no cyano substituents (NCC and NCT, Figure 1C) as our putative mechanophores. These particular cyclobutanes were chosen for their variation in not only the degree of substitution but also for their variation in the relative stereochemistry (cis and trans) of the pendant ester groups as well as the electronics of the cyclobutane ring. This set of structures provided an appropriate level of diversity for an initial foray into the development of both computational and mechanochemical testing protocol for SMAR.

Before the synthesis of this series of mechanophores was attempted, a sequence of CoGEF calculations was carried out to predict the trends of fragmentation reactivity. CoGEF is a computational method developed by Beyer that probes the effect of molecular stretching deformations upon fragmentation reactions.[38] By artificially constraining the distance between two points (i.e., two atoms) in the structure of a mechanophore and sequentially increasing the distance between these points by discrete increments, it is possible to simulate the effects of induced molecular-scale mechanical deformation in a controlled way. In the case of the mechanophores studied herein, by sequentially increasing the distance between the methyl carbons of the methyl ester groups and measuring the corresponding change in ground state energy, it is possible to estimate the energy necessary to fragment a particular mechanophore (see Supporting Information for details). The relationship of this CoGEF energy to activation energy is unclear, but one might anticipate the two to be strongly correlated. An example of a CoGEF elongation energy curve for the DCC mechanophore can be found in Figure 2 above. Starting from the unconstrained, energy minimized structure, elongation results in stretching of the molecule and an increase in the

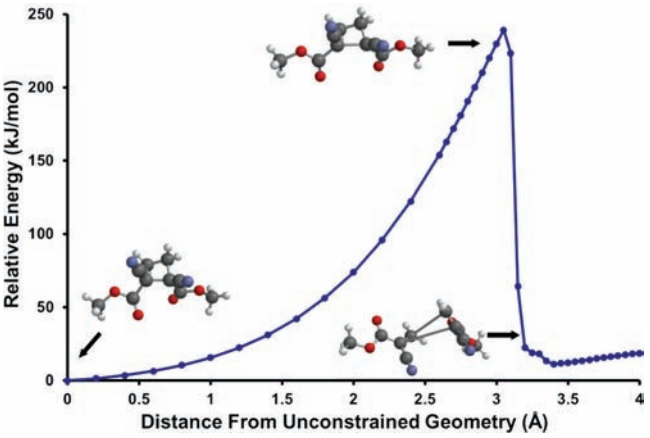

Figure 2. CoGEF results for the DCC mechanophore. Upon pulling apart the methyl ester groups, the molecule first elongates then abruptly fragments into a pair of alkenes (all CoGEF calculations were done using a DFT-B3LYP 6-31G* level of theory).

Table 1. CoGEF, F_{max}, and Cleavage Threshold Values for Mechanophores Studied Herein

mechanophore	CoGEF (kJ/mol)	F_{max}[a] (nN)	threshold (kDa)
DCC	239	3.30	11.7
DCT	266	5.03	23.5
MCC	269	3.67	23.9
MCT	275	4.72	29.3
NCC	336	4.37	23.6
NCT	386	5.90	33.9

[a] F_{max} values were calculated using the method outlined in ref 38.

ground-state energy. At the peak of the curve (energy maximum), the cyclobutane fragments and then relaxes to a lower energy conformation, where a retro [2 + 2] reaction has occurred to form two alkenes. In the case of all six of the cyclobutanes, molecular elongation resulted in a retro [2 + 2] reaction with the formation of two alkenes.

In the cases studied herein, it should be noted that the molecular forces induced during CoGEF calculations directly affect the bond that is expected to cleave. There may be cases where the expected mechanophore activation results from very different reaction geometries or mechanisms (for example, mechanophores that would activate through bond rearrangements without concurrent chain scission). In these cases, an alternative modeling method may be more appropriate, however, the concepts introduced herein should still hold true.

Upon completion of these CoGEF calculations for all six mechanophores (Table 1), two trends in the relative fragmentation energy emerged. The first trend noted was that for a given level of substitution, the cis mechanophore was more reactive than the trans mechanophore (for example, DCC was more reactive than DCT). This trend can also be seen in the F_{max} values (Table 1) calculated for these mechanophores, where F_{max} is the maximum force imposed on the model mechanophores for bond rupture to occur. We speculate that this difference in reactivity is possibly due to steric interactions between pendant ester groups within the cis diester that are not present in the trans diester.

The second trend was that mechanophore reactivity increased as the level of mechanophore substitution increased (for example,

Scheme 1. Synthesis of Cyclobutane Mechanophore Cores[a]

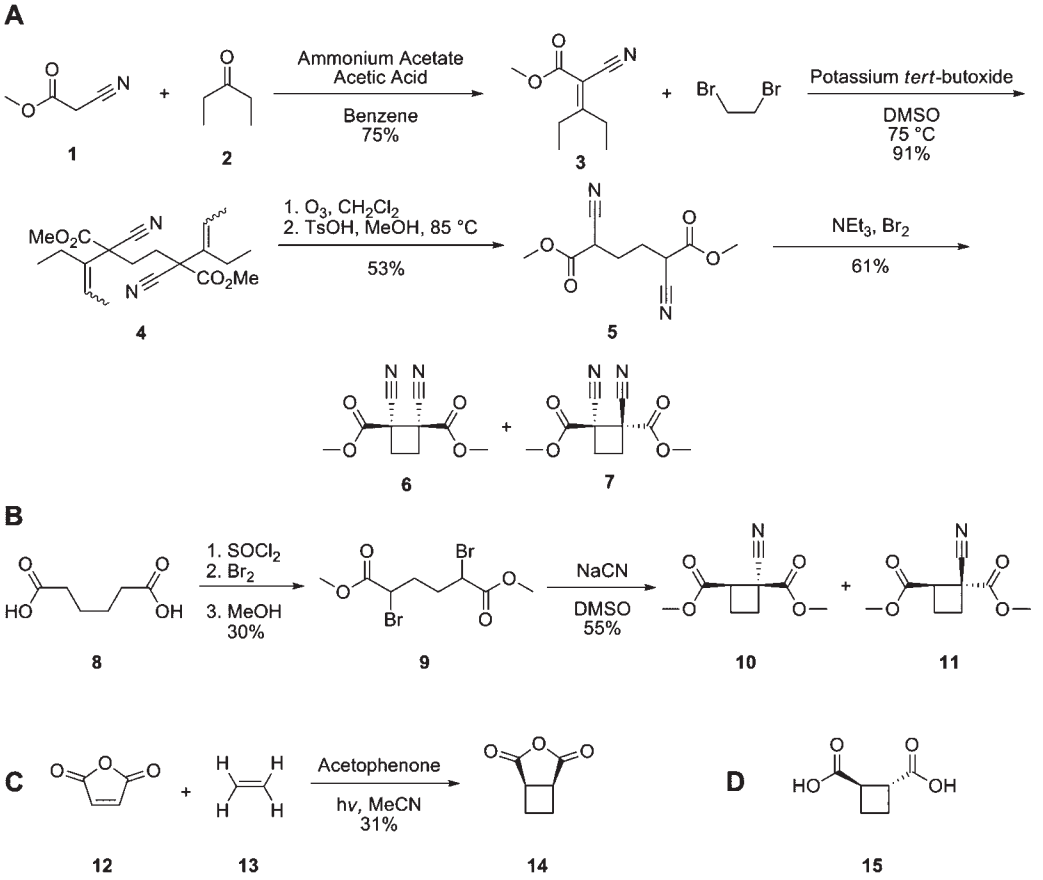

[a] (A) Synthesis of dimethyl ester-DCC and dimethyl ester-DCT. (B) Synthesis of dimethyl ester-MCC and dimethyl ester-MCT. (C) Synthesis of 3-oxabicyclo[3.2.0]heptane-2,4-dione (NCC core). (D) Commercially available *trans*-cyclobutane-1,2-dicarboxylic acid (NCT core).

DCT was more reactive toward cleavage than MCT, which in turn was more reactive than NCT). We speculate this higher reactivity is a result of increased steric interactions upon the 1,2-substituted cyclobutane bond, which leads to increased ring strain. This notion is supported by analyzing the average bond lengths of the 1,2-substituted structures;[42] whereby longer bond lengths reflect greater internal ring strain and increased susceptibility to cyclobutane cleavage. The average 1,2-cyclobutane bond length for the dicyano-substituted cyclobutanes was 1.61 Å, whereas the average 1,2-cyclobutane bond length for the monocyano-substituted cyclobutanes was 1.58 Å. Finally, bond lengths averaged 1.55 Å for cyclobutanes having no cyano substituents. Concurrently, this additional reactivity could also be a result of increased stabilization of the transition states leading to diradical intermediates that are formed during asynchronous cyclobutane fragmentation.[21] Regardless of the reasoning, we show below that the predicted trends are testable through the synthesis of a polymer molecular weight series for each of the cyclobutane derivatives followed by a statistical comparison of their rates of fragmentation in an acoustic field.

In order to test the computational results, all six of the cyclobutanes were synthesized. The cis and the trans dicyano-substituted cyclobutanes were synthesized starting with the commercially available methyl cyanoacetate **1** and 3-pentanone **2**.[21] A Knoevenagel condensation of these two starting materials resulted in α,β-unsaturated ester **3**,[43] which was reacted with dibromoethane to yield a mixture of bis-alkenes **4**. Ozonolysis followed directly by methanolysis yielded the symmetric dicyano diester **5**. Ring closure gave a mixture of methyl ester substituted cyclobutanes **6** (DCC) and **7** (DCT) in a 1:3 ratio. The products were further separated to give the pure isomers via sublimation (Scheme 1A), where relative stereochemistry was determined through X-ray crystallography (see Supporting Information). Enantiomers of **7** were tested as a racemic mixture of the DCT mechanophore. MCC and MCT were synthesized by α-bromination and methyl-esterification of adipic acid **8** to yield diester **9**.[44] This step was followed by the addition of sodium cyanide to afford a racemic mixture of cyclobutanes **10** (MCC) and diastereomer **11** (MCT), which were further separated through selective crystallization of the cis derivative (Scheme 1B). The structure of MCC was confirmed by X-ray crystallography (see Supporting Information). The NCC mechanophore was synthesized from the [2 + 2] cycloaddition of ethylene gas and maleic anhydride to form 3-oxabicyclo-[3.2.0]heptane-2,4-dione[45] **14** (Scheme 1C), and the NCT mechanophore was synthesized from the commercially available enantiomeric mixture of *trans*-cyclobutane-1,2-dicarboxylic acid **15** (Scheme 1D).

After successful synthesis of the mechanophores, the installation of initiator groups was necessary for the growth of pendant polymer chains via single-electron-transfer living radical polymerization (SET-LRP).[46] This installation of initiator groups was accomplished through transesterification of the mechanophores

dx.doi.org/10.1021/ja2086728 |*J. Am. Chem. Soc.* 2011, 133, 18992–18998

Scheme 2. General Synthesis of Initiator Functionalized Mechanophores and Control for the Formation of Chain-Centered PMA

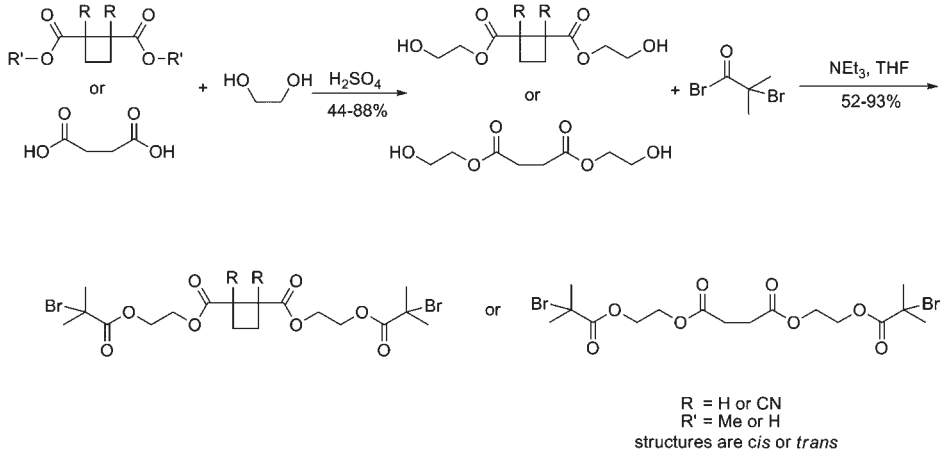

with ethylene glycol to form the bis-hydroxy functionalized derivatives followed by reaction with α-bromoisobutyryl bromide to install the needed α-bromoester functionalized initiators for polymerization (Scheme 2). In addition to these mechanophore-containing initiators, two control initiators were used. The first of these (CON1) consisted of a simple alkane bridge to replace the active cyclobutane mechanophores. This initiator was synthesized in a manner similar to the mechanophore initiators above (Scheme 2). Additionally, the simple monofunctional initiator methyl 2-bromopropionate was used in the synthesis of homopolymer containing no center-functionalized mechanophore or alkane bridge as a second control (CON2).

From these eight unique initiators (six active mechanophore initiators as well as two control initiators) was produced a series of center- or end-functionalized polymers of varying molecular weight. Specifically, a series of low polydispersity (PDI) poly(methyl acrylate) (PMA) polymers ranging from 35 to 125 kDa was synthesized using SET-LRP (see Supporting Information for specific molecular weights and PDIs). The molecular weight series of center-functionalized polymers containing the various mechanophores makes it possible to probe relative reactivities by measuring the relative rates of mechanophore scission in an acoustic field.[21] Molecular weight values, which were critical for the analysis described below, were measured by gel permeation chromatography (GPC) and are calculated relative to monodisperse polystyrene standards.

In order to determine the relative rates of polymer cleavage, dilute solutions of polymer were exposed to ultrasonic irradiation at a controlled temperature (6−9 °C) under an argon atmosphere. During each sonication, aliquots were removed at regular intervals and were subsequently analyzed by GPC. Every sonication experiment was performed in duplicate to ensure reproducibility.

Rates of molecular cleavage can be calculated using the method utilized by Malhotra and co-workers.[47,48] Based on the assumption that, during mechanical cleavage, random chain scission occurs along the backbone of the polymer, Malhotra used the theoretically derived[49−51] eq 1 to model time-dependent change in molecular weight:

$$\frac{1}{M_t} = \frac{1}{M_i} + k't \qquad (1)$$

where $k' = k/M_0$, M_0 is the molecular weight of the monomer unit, M_i is the initial number average molecular weight (M_n) of the polymer, M_t is the number average molecular weight of the sonicated sample at time t, and k is the rate constant of polymer cleavage with initial molecular weight M_i. While the aforementioned model assumes random scission along the backbone of the polymer, it has been shown to also be applicable to systems where center-selective scission is taking place (as is the case with polymers sonicated in solution).[21,47] Each of the mechanophore-containing polymers was exposed to ultrasonic irradiation, and the change in molecular weight distribution as a function of ultrasound irradiation time was recorded by GPC (see example, Figure 3A). A plot of the number average molecular weight values obtained by GPC vs ultrasonic irradiation time shows an asymptotic decay profile (Figure 3B). The cleavage rate constant (k) for a mechanophore at a given initial molecular weight is calculated by nonlinear least-squares fitting of eq 1 to this data. As shown in Figure 3B, the fitted decay profile (solid curve) is in good agreement with the experimental data (points). A similar procedure was used to calculate the rate constant for each polymer synthesized.

It is well-known that there is a molecular weight dependence in the rate of polymer scission induced by sonication.[4] Longer polymer chains result in faster rates of cleavage. As long as the initial molecular weight is not above ca. 150 kDa, a linear relationship has empirically been found between molecular weight and cleavage rate. Additionally, there is a molecular weight threshold below which polymer chains do not fragment under sonication conditions.[3] Our group has previously shown that inclusion of a single chain-centered mechanophore in the polymer backbone lowers the molecular weight threshold due to selective cleavage of the mechanophore.[29] By comparing the sonochemically determined thresholds for the different mechanophores synthesized, we can investigate the relationship between mechanophore structure and reactivity. This comparison should allow us to test the effectiveness of CoGEF calculations in predicting mechanochemical trends.

Comparison of rate values was accomplished by sonicating all eight of the unique polymer molecular weight series. Using the method of Malhotra and co-workers outlined above, the rates of cleavage were determined for each polymer of initial molecular weight M_i for each of the different mechanophores and the control polymers. The differences in mechanophore reactivity are best seen in plots of k vs M_i. As described below, the different mechanophores result in changes in threshold molecular weight

dx.doi.org/10.1021/ja2086728 |J. Am. Chem. Soc. 2011, 133, 18992–18998

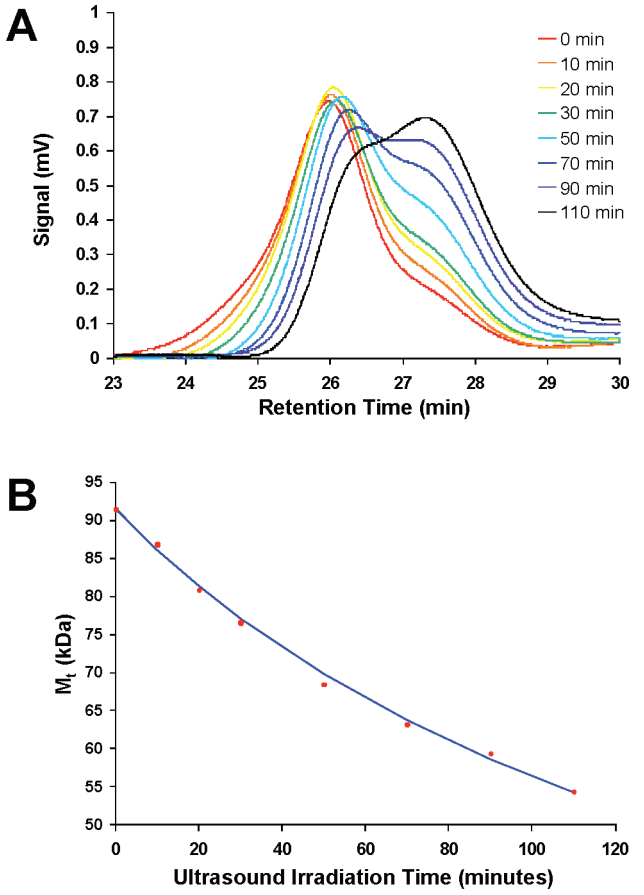

Figure 3. GPC traces and modeled data depicting the effect of ultrasonic irradiation on a mechanophore containing polymer. A 0.75 mg/mL solution of polymer in acetonitrile was subjected to ultrasound at 20 kHz, 8.7 W/cm^2, and 6−9 °C under argon (0.5 s on, 1.0 s off; irradiation time refers to total time both off and on). (A) Change in GPC trace for a sonicated DCT polymer having an M_i of 90 kDa. The inset colors code the samples according to ultrasound irradiation time. (B) Experimentally obtained number average molecular weight (M_t) with respect to time of sonication (data points) and best fit (solid curve) to the Malhotra model. The curve was derived by adjusting the k' value in eq 1 to the experimental data using a nonlinear least-squares fitting routine.

(i.e., x-axis intercept, also called elevation) rather than slope (Table 1). Specifically, it was found that the rate of change due to molecular weight differences was not statistically different for any of the polymer series studied (see Supporting Information for details).[52]

Most importantly, we wanted to know whether the changes in molecular weight threshold were significantly different for each of the mechanophore-containing polymers. Using the statistical method outlined by Zar, it was found that many of the perceived differences in threshold were in fact statistically significant at the 95% confidence value (see Supporting Information for detailed statistical analysis and t-test values).[52] Thus, an important general conclusion from this study is that the inclusion of a single, center-linked mechanophore results in measurable and statistically significant shifts in molecular weight thresholds for polymer cleavage. As detailed below, these threshold molecular weight differences depend on the specific structure of the mechanophore, which correlate favorably to reactivity trends predicted by CoGEF calculations.

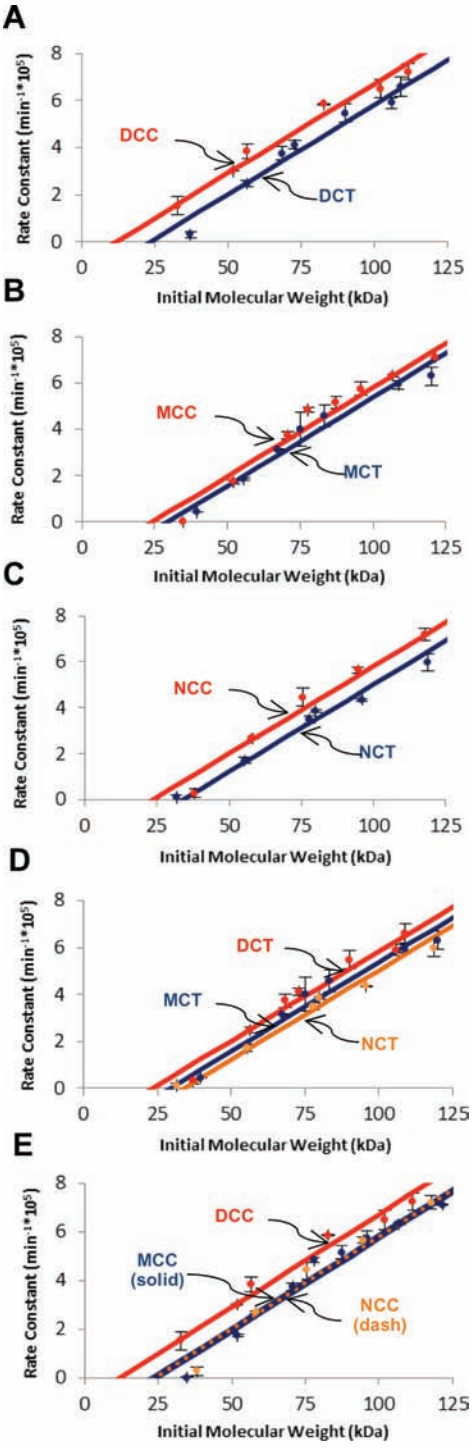

Figure 4. Experimentally determined rate constants of polymer cleavage as a function of initial polymer molecular weight, R^2 values for the fit lines are included in parentheses. (A) Cleavage of DCC (R^2 = 0.974) and DCT (R^2 = 0.962) polymers. (B) Cleavage of MCC (R^2 = 0.958) and MCT (R^2 = 0.961) polymers. (C) Cleavage of NCC (R^2 = 0.965) and NCT (R^2 = 0.972) polymers. (D) Cleavage of DCT, MCT, and NCT polymers. (E) Cleavage of DCC, MCC, and NCC polymers.

The first trend analyzed was the relationship between stereochemistry and reactivity. CoGEF calculations predicted that the cis derivatives would be more reactive than the trans derivatives for a given level of substitution. In comparing the DCC mechanophore

to the DCT mechanophore (Figure 4A), there was a statistically significant threshold molecular weight difference, with the DCC mechanophore being more reactive (i.e., smaller *x*-axis intercept value). This result is seen by the higher elevation of the fitted line for the cis derivative in the plot of k vs M_i. This means that, for a given molecular weight, a polymer containing the DCC mechanophore cleaves faster than a polymer containing the DCT mechanophore, and consequently, the DCC mechanophore is more mechanochemically reactive. Comparing MCC and MCT, the cis mechanophore again appears, by visual inspection of the plot, to be more reactive; however, the difference in the intercepts was not statistically significant at the 95% confidence interval (Figure 4B). On the other hand, the NCC mechanophore, using the statistical criterion outlined above, was more reactive than the NCT mechanophore, consistent with the CoGEF calculations (Figure 4C).

The relationship between level of cyclobutane substitution and mechanophore reactivity was the second trend analyzed. CoGEF calculations predicted that the more highly substituted mechanophores will cleave more readily than the less-substituted derivatives; this behavior is presumably due to increased ring strain present within the cyclobutane rings in the higher-substituted derivatives, which is consistent with the ring's carbon−carbon bond lengths. Upon analysis of the trans series of mechanophores (Figure 4D), we found that this trend was indeed the case. By comparison of threshold values, the DCT mechanophore was the most reactive, followed by the MCT mechanophore, and finally, the NCT mechanophore was the least reactive. Analyzing the cis series, the trend in reactivity is less clear. The DCC mechanophore is significantly more reactive than the MCC and NCC mechanophores; however, threshold values for the latter two are statistically indistinguishable from each other (Figure 4E). Nonetheless, the general reactivity trends concerning degree of substitution predicted through CoGEF are, again, generally validated by the rate data presented in Figure 4.

The mechanophore-containing polymers were also compared to the control polymers that were synthesized in order to verify that they were indeed more reactive than polymers that did not contain a cyclobutane ring in the center (CON1) as well as simple PMA homopolymers (CON2). Based on statistical comparison of threshold values, it was found that all of the cyclobutane mechanophores studied herein are more reactive than the control polymers, with the exception of the NCT mechanophore. As the least reactive of the mechanophores, the NCT derivative had threshold molecular weights that were statistically indistinguishable from the thresholds of both CON1 and CON2. Consequently, it is plausible that the polymers containing the NCT mechanophore are not selectively cleaved at the cyclobutane moiety (possibly due to the decreased internal ring strain present in the NCT mechanophore when compared to the other cyclobutanes). General and unselective chain scission of the polymer backbone is likely occurring in addition to cleavage of the mechanophore in the case of NCT (See Supporting Information for details).

CONCLUSIONS

The development of mechanically activated small molecules (i.e., mechanophores) with targeted molecular level responses is a relatively new field of study that has only come to prominence in the last five years.[3] Although many interesting and potentially useful mechanophores have been developed, few systematic studies have been conducted that combine computational and experimental approaches toward predicting trends in reactivity. Herein, we illustrate the SMAR method for investigating these trends. By probing the effects of mechanophore structure through the systematic study of a class of putative mechanophores, our aim is to open the way for the rational design and development of new mechanically activated molecules.

The systematic synthesis and study of a molecular weight series of cyclobutane-containing polymers experimentally validated CoGEF as a computational tool for the investigation of SMARs. Both stereochemical and substitutional reactivity trends in a series of mechanophores were predicted using CoGEF, and the trends were compared to the behavior of a series of center-functionalized polymers that fragment when subjected to an acoustic field. Plots of cleavage rate constant vs initial molecular weight gave threshold molecular weight values that differed in a statistically significant way for many of polymers, even though each macromolecule contains just one cyclobutane mechanophore. The trends in threshold molecular weight generally agreed with reactivity predicted by CoGEF calculations.

ASSOCIATED CONTENT

Supporting Information. Experimental details, synthetic procedures, GPC data, statistical analysis, crystallographic data, and details on computational modeling. This material is available free of charge via the Internet at http://pubs.acs.org.

AUTHOR INFORMATION

Corresponding Author
jsmoore@illinois.edu

ACKNOWLEDGMENT

This work was supported by the Army Research Office MURI (grant W911NF-0701-0409). The authors thank Koushik Ghosh, Preston May, and Doug Davis for helpful discussions relating to this project.

REFERENCES

(1) *GlaxoSmithKline Common Questions Website*; http://us.gsk.com (accessed August 13, 2011).
(2) Peltason, L.; Bajorath, J. *J. Med. Chem.* **2007**, *50*, 5571.
(3) Caruso, M. M.; Davis, D. A.; Shen, Q.; Odom, S. A.; Sottos, N. R.; White, S. R.; Moore, J. S. *Chem. Rev.* **2009**, *109*, 5755.
(4) Basedow, A. M.; Ebert, K. H. *Adv. Polym. Sci.* **1977**, *22*, 83.
(5) Nguyen, T. Q.; Kausch, H.-H. *Adv. Polym. Sci.* **1992**, *100*, 73.
(6) Rubner, M. F. *Macromolecules* **1986**, *19*, 2129.
(7) Nallicheri, R. A.; Rubner, M. F. *Macromolecules* **1991**, *24*, 517.
(8) Beyer, M. K.; Clausen-Schaumann, H. *Chem. Rev.* **2005**, *105*, 2921.
(9) Schmidt-Naake, G.; Drache, M.; Weber, M. *Macromol. Chem. Phys.* **2002**, *203*, 2232.
(10) Devries, K. L.; Roylance, D. K.; Williams, M. L. *J. Polym. Sci, Part B: Polym. Phys.* **1972**, *10*, 599.
(11) Devries, K. L.; Roylance, D. K.; Williams, M. L. *J. Polym. Sci, Part A: Polym. Chem.* **1970**, *8*, 237.
(12) Sohma, J. *Prog. Polym. Sci.* **1989**, *14*, 451.
(13) Encina, M. V.; Lissi, E.; Sarasúa, M.; Gargallo, L.; Radic, D. *J. Polym. Sci. Polym. Lett. Ed.* **1980**, *18*, 757.
(14) Sheiko, S. S.; Sun, F. C.; Randall, A.; Shirvanyants, D.; Rubinstein, M.; Lee, H.-I.; Matyjaszewski, K. *Nature* **2006**, *440*, 191.

(15) Zysman, V.; Nguyen, T. Q.; Kausch, H.-H. *J. Polym. Sci, Part B: Polym. Phys.* **1994**, *32*, 1257.
(16) Beiermann, B. A.; Davis, D. A.; Kramer, S. L. B.; Moore, J. S.; Sottos, N. R.; White, S. R. *J. Mater. Chem.* **2011**, *21*, 8443.
(17) Kingsbury, C. M.; May, P. A.; Davis, D. A.; White, S. R.; Moore, J. S.; Sottos, N. R. *J. Mater. Chem.* **2011**, *21*, 8381.
(18) Lee, C. K.; Davis, D. A.; White, S. R.; Moore, J. S.; Sottos, N. R.; Braun, P. V. *J. Am. Chem. Soc.* **2010**, *132*, 16107.
(19) Davis, D. A.; Hamilton, A.; Yang, J.; Cremar, L. D.; Van Gough, D.; Potisek, S. L.; Ong, M. T.; Braun, P. V.; Martínez, T. J.; White, S. R.; Moore, J. S.; Sottos, N. R. *Nature* **2009**, *459*, 68.
(20) Potisek, S. L.; Davis, D. A.; Sottos, N. R.; White, S. R.; Moore, J. S. *J. Am. Chem. Soc.* **2007**, *129*, 13808.
(21) Kryger, M. J.; Ong, M. T.; Odom, S. A.; Sottos, N. R.; White, S. R.; Martinez, T. J.; Moore, J. S. *J. Am. Chem. Soc.* **2010**, *132*, 4558.
(22) Black, A. L.; Orlicki, J. A.; Craig, S. L. *J. Mater. Chem.* **2011**, *21*, 8460.
(23) Wiggins, K. M.; Hudnall, T. W.; Shen, Q.; Kryger, M. J.; Moore, J. S.; Bielawski, C. W. *J. Am. Chem. Soc.* **2010**, *132*, 3256.
(24) Wiggins, K. M.; Syrett, J. A.; Haddleton, D. M.; Bielawski, C. W. *J. Am. Chem. Soc.* **2011**, *133*, 7180.
(25) Hickenboth, C. R.; Moore, J. S.; White, S. R.; Sottos, N. R.; Baudry, J.; Wilson, S. R. *Nature* **2007**, *446*, 423.
(26) Lenhardt, J. M.; Ong, M. T.; Choe, R.; Evenhuis, C. R.; Martinez, T. J.; Craig, S. L. *Science* **2010**, *329*, 1057.
(27) Tennyson, A. G.; Wiggins, K. M.; Bielawski, C. W. *J. Am. Chem. Soc.* **2010**, *132*, 16631.
(28) Karthikeyan, S.; Potisek, S. L.; Piermattei, A.; Sijbesma, R. P. *J. Am. Chem. Soc.* **2008**, *130*, 14968.
(29) Berkowski, K. L.; Potisek, S. L.; Hickenboth, C. R.; Moore, J. S. *Macromolecules* **2005**, *38*, 8975.
(30) Huang, Z.; Yang, Q.-Z.; Khvostichenko, D.; Kucharski, T. J.; Chen, J.; Boulatov, R. *J. Am. Chem. Soc.* **2009**, *131*, 1407.
(31) Yang, Q.-Z.; Huang, Z.; Kucharski, T. J.; Khvostichenko, D.; Chen, J.; Boulatov, R. *Nat. Nanotechnol.* **2009**, *4*, 302.
(32) Ong, M. T.; Leiding, J.; Tao, H.; Virshup, A. M.; Martínez, T. J. *J. Am. Chem. Soc.* **2009**, *131*, 6377.
(33) Lenhardt, J. M.; Ogle, J. W.; Ong, M. T.; Choe, R.; Martinez, T. J.; Craig, S. L. *J. Am. Chem. Soc.* **2011**, *133*, 3222.
(34) Dopieralski, P.; Ribas-Arino, J.; Marx, D. *Angew. Chem., Int. Ed.* **2011**, *50*, 7105.
(35) Dopieralski, P.; Anjukandi, P.; Rückert, M.; Shiga, M.; Ribas−Arino, J.; Marx, D. *J. Mater. Chem.* **2011**, *21*, 8309.
(36) Ribas-Arino, J.; Shiga, M.; Marx, D. *J. Am. Chem. Soc.* **2010**, *132*, 10609.
(37) Ribas-Arino, J.; Shiga, M.; Marx, D. *Angew. Chem., Int. Ed.* **2009**, *48*, 4190.
(38) Beyer, M. K. *J. Chem. Phys.* **2000**, *112*, 7307.
(39) Schmidt, S. W.; Beyer, M. K.; Clausen-Schaumann, H. *J. Am. Chem. Soc.* **2008**, *130*, 3664.
(40) Cho, S.-Y.; Kim, J.-G.; Chung, C.-M. *Sens. Actuators, B* **2008**, *134*, 822.
(41) Chung, C.-M.; Roh, Y. S.; Cho, S. Y.; Kim, J. G. *Chem. Mater.* **2004**, *16*, 3982.
(42) Bond Lengths were determined from crystal structures in the case of DCC, DCT, and MCC. Due to MCT, NCC, and NCT being liquids, bond lengths were calculated using a computational minimization of their structures (see Supporting Information for details).
(43) Cope, A. C.; Hofmann, C. M.; Wyckoff, C.; Hardenbergh, E. *J. Am. Chem. Soc.* **1941**, *63*, 3452.
(44) Guha, P. C.; Sankaran, D. K. *Org. Syn.* **1946**, *26*, 57.
(45) Faure, S.; Jensen, A. A.; Maurat, V.; Gu, X.; Sagot, E.; Aitken, D. J.; Bolte, J.; Gefflaut, T.; Bunch, L. *J. Med. Chem.* **2006**, *49*, 6532.
(46) Percec, V.; Guliashvili, T.; Ladislaw, J. S.; Wistrand, A.; Stjerndahl, A.; Sienkowska, M. J.; Monteiro, M. J.; Sahoo, S. *J. Am. Chem. Soc.* **2006**, *128*, 14156.
(47) Malhotra, S. *J. Macromol. Sci., Part A* **1986**, 37.
(48) Malhotra, S. *J. Macromol. Sci., Part A* **1982**, *18*, 1055.
(49) Sato, T.; Nalepa, D. E. *J. Appl. Polym. Sci.* **1978**, *22*, 865.
(50) Casassa, E. *J. Polym. Sci.* **1949**, *4*, 405.
(51) Jellinek, H. H. G. *J. Polym. Sci.* **1949**, 264.
(52) Zar, J. H. Comparing Simple Linear Regression Equations. Biostatistical Analysis, 5th ed.; Pearson Prentice Hall: Upper Saddle River, NJ, 2010; p 363.